Bulgarian Chemical Communications, Special Edition H, (pp. 19 – 24) 2017

Thermally induced pore pressure and consolidation volumetric strain for saturated soils

B. Bai[1*], S. Jiang[1]

[1] *School of Civil Engineering, Beijing Jiaotong University, Beijing 100044, PR China*

Received June 19 2017, Revised July 20 2017

The aim of this paper is to experimentally investigate thermally induced pore pressure and subsequent consolidation volumetric strain. Studies show that normalized pore pressure tends to decrease with an increase in confining pressure and repeated thermal loading cycles. Test results from three typical soils all show that there are approximately linear relationships between consolidation volumetric strain and thermally induced pore pressure, which is influenced by the specimens' water content, confining pressure, and amplitude, and the number of thermal loading cycles applied. An equation for describing the pore pressure induced by temperature and confining pressures is proposed. Additionally, the relationship between consolidation volumetric strain and thermally induced pore pressure is established.

Key words: Thermal energy, Induced pore pressure, saturated soil, repeated thermal loading, Geo-environmental influence.

INTRODUCTION

Soil thermal properties are encountered in many engineering fields dealing with high-level nuclear waste isolation, waste containment facilities, gas pipelines, energy piles, electric transmission lines, thermal ground improvement techniques, etc. [1, 2]. Much effort has been made to model heat transfer through geomaterials with the help of experimental, analytical or numerical models [3]. Hüpers and Kopf [4] have discussed thermal influence on the consolidation state of oceanic sediments and its implications for excess pore pressure, with increasing temperature leading to an enhanced reduction in pore space. Due to the need for a barrier material in nuclear waste disposal repositories, Villar et al [5] experimentally investigated the dependence of the swelling strains of bentonite on temperature, the increase in permeability of water-saturated bentonite with increased temperature, water retention curves of bentonite compacted at different dry densities, among other effects. Bai and Chen [6] have discussed the degradation effect of saturated clay subjected to cyclic thermal loading using a temperature-controlled triaxial apparatus.

The temperature increases in saturated porous materials under undrained conditions may lead to thermal pressurization of the pore fluid. This increase in the pore fluid pressure induces a reduction of the effective mean stress, and can lead to shear failure or hydraulic fracturing. Khalili et al [7] have presented a non-isothermal constitutive relation for a saturated porous material, derived a closed-form solution for the heat-induced pore pressure, and examined the validity of the theoretical assertions through a targeted program of laboratory testing as well as data from the literature. Ghabezloo and Sulem [8] believe that the thermally induced pore pressure is determined by the discrepancy between the thermal expansion of the pore fluid and of the solid phase, the stress-dependency of the compressibility and the non-elastic volume changes of the porous material. Monfared et al [9] have discussed the thermal pore pressure of low-permeability argillites using a hollow cylinder triaxial cell. Yilmaz [10] has investigated the thermal impact on particle size, water content, specific gravity, plasticity, activity index, swelling characteristics, compression index and strength properties, specifically for kaolinite and bentonite.

The thermal behavior of soils, including pore pressure and thermal deformation, is a function of mineralogical composition, porosity, pore fluid, degree of saturation, water content, range of temperature change, state of stress, and other factors [11]. Laloui and Cekerevac [12] have discussed the combined effects of some factors in both drained and undrained conditions. Ouhadi et al [13] have investigated the impact of temperature on the re-structuring of the soil microstructure, as well as its geotechnical and geo-environmental influences on smectite behavior. However, the thermal behaviors of soils are not yet completely understood in extant literatures. For instance, the undrained thermal pressurization coefficient differs by two orders of magnitude in some studies [14, 15].

* To whom all correspondence should be sent:
E-mail: baibing66@263.net

At present, reliable assessment methods for pore pressure induced by heating and subsequent consolidation deformation due to dissipation of the pore pressure are scarce. In this study, thermally induced pore pressure and subsequent consolidation volumetric strain is experimentally investigated using three typical soils, and the influence factors such as specimens' water content, confining pressure, amplitude, and number of thermal loading cycles are discussed. Finally, methods for describing the pore pressure and consolidation volumetric strain with pore pressure are proposed.

TEST DESCRIPTIONS

Test soils

This test includes three types of soils. The physical properties are as follows: soil 1 is a silty clay, with specific gravity G_S=2.71, plastic limit w_P=17.6%, liquid limit w_L=31.4%, and plasticity index I_P=13.8; soil 2 is a clay, with G_S=2.71, w_P=15.8%, w_L=34.9%, and I_P=19.1; soil 3 is a red clay, with G_S=2.74, w_P=39.2%, w_L=71.8%, I_P=32.6. These soils were chosen for analysis because they have very distinct plasticity indexes. Soil 1 (silty clay) and soil 2 (clay) were taken from Beijing, China, and soil 3 (red clay; i.e., laterite) was taken from Guangxi, China. To obtain uniform samples, air-dried sediments were groundto soil fines that could pass through a 0.5 mm sieve. The soils were mixed to predetermined initial water contents and stored in a plastic container. After at least 24 hours, the sample was taken out and poured into a cylindrical specimen mold. The prepared specimens were 3.91 cm in diameter and 8 cm in height. Next, the molds, together with the specimens, were placed in a large vessel for saturation by vacuum pump for at least 6 hours, and finally were immersed in distilled water for testing.

In all of the tests, vertical strips of filter paper were placed on the sides of the specimen to speed up the consolidation. Additionally, filter paper discs were positioned on the top and bottom of the soil specimens to prevent particles from being forced into the pores of the porous stones placed on the specimen ends. Before this, the porous stones were kept in distilled water and then boiled for sufficient time to reach saturation.

Test apparatus

Tests were performed using a triaxial shear device modified for the thermal loading application, which was described in reference [6]. The temperature inside the pressure chamber can vary in the 20 ºC-100 ºC range, controlled by an electro-thermal belt inside the metallic hollow sleeve of the chamber, which is connected to a thermocouple. The precision of the thermo-controller system is ±0.1 ºC. The pore pressure was measured through a porous stone at the bottom center of the specimens, using a pore pressure transducer (measuring range: 0-1 MPa) connected to a digital monitoring apparatus. Pore pressure measurement was resolved to 0.1 kPa. The confining pressure was also monitored and controlled using a pressure transducer (measuring range: 0-1 MPa) attached to the bottom of the pressure chamber by another digital monitoring apparatus.

Test methods

Table 1 gives the test schemes (cases 1, 2, 3 and 4), the brief descriptions of which are as follows:

Case 1 and 2

For soil 1 (the remolded saturated silty clay), several undrained heating tests are conducted. This scheme includes two water content levels (w=25.1% and 22.1%; Case 1 and 2 in Table 1, respectively), three confining pressures (σ'_3=50, 100, and 150 kPa), six heating-cooling cycles and two thermal loading amplitudes (θ=25 ºC and 50 ºC). The thermal loading amplitude is expressed here as $\theta=T-T_0$, where T and T_0 are the current and initial temperatures, respectively.

The specimens were isotropically consolidated under different effective confining pressures at a primary temperature of T_0=25 ºC. With the completion of the isotropical consolidation, the specimens were then subjected to six heating-cooling cycles, with each cycle (N=1, 2, 3, 4, 5, 6) consisting of undrained heating from the primary temperature of 25 ºC to a higher temperature of 50 ºC, isothermal consolidation at the elevated temperature of 50 ºC, undrained cooling from 50 ºC to 25 ºC, and isothermal consolidation (a drainage or water-absorbing process) at the original temperature of 25 ºC. This composed a single cycle of the heating-cooling process. Next, the heating-cooling process was repeated.

Case 3

For soil 2 (i.e., the remolded saturated clay), specimens were isotropically consolidated under various effective confining pressures σ'_3 (σ'_3=50, 100, and 150 kPa) at a primary temperature of T_0=20 ºC, and then heated to a higher temperature in two steps (20 ºC→50 ºC→80 ºC) under undrained conditions. The specimen temperature is then lowered again in two steps (80 ºC→50 ºC →20 ºC). During heating and cooling, the

specimens are not allowed to dissipate; the specimens are heated to a given higher temperature (50 ºC or 80 ºC), and then allowed to consolidate (a drainage or water-absorbing process). After this, the heating-cooling process was repeated a second and third time.

Case 4

For soil 3 (the remolded red clay), specimens were isotropically consolidated under the effective confining pressure of σ'_3=50 kPa and primary temperature T_0=20 ºC, and then heated to a different higher temperature (T=40, 50, 60, 80, 90 ºC; see Table 1) under undrained conditions. The specimens were then allowed to consolidate.

THERMALLY INDUCED PORE PRESSURS

Pore pressure during repeated undrained heating

Figure 1 gives the relationship between normalized pore pressure u/σ'_3 and temperature T for three confining pressures (σ'_3=50, 100, and 150 kPa) during repeated undrained heating and cooling when θ=25 ºC and θ=50 ºC, respectively. Test results show that the normalized pore pressure increases as the temperature of the specimen increases during undrained heating. Generally, the normalized pore pressure decreases with the increase in confining pressure, which can be seen in comparisons between Fig. 1(a), (b), and (c) or Fig. 1(d), (e), and (f). Additionally, the pore pressure appears to degrade with increasing temperature cycles (N=1, 2, 3, 4, 5 and 6). With the increase in confining pressure and repeated thermal loading cycles, the ranges of variation of pore pressure narrow during subsequent heating and cooling processes, which reflects an “aging effect” of saturated soils due to heating. At this time, the soils will show an over-consolidated state. In other words, the specimens initially exhibit an obvious un-recovered thermo-mechanical process at a normally consolidated or lightly over-consolidated state, and eventually transition to a recovered thermo-elastic response at a heavily over-consolidated state with cyclic thermal loading.

It should be noted that with increasing temperature, the thermal pore pressure takes on a complicated non-linear evolution process, which is closely related to the physical properties of the soil, confining pressure, number of thermal loading cycles, and the overconsolidation ratio of the soil. When the specimen temperature is lower (T<50 ºC; see Fig. 1(a), (b), (c)), the undrained thermal pressurization coefficient, defined as the pore pressure variation due to a unit temperature variation in the undrained condition, increases with the increase in temperature; however, under a higher temperature and a lower confining pressure (T>60 ºC and σ'_3=50 kPa; see Fig. 1(d)), the undrained thermal pressurization coefficient initially increases and then gradually begins to decrease.

On the other hand, the pore pressure decreases during undrained cooling processes (50→25 ºC in Fig. 1), and the undrained thermal pressurization coefficient also decreases. The shape of the temperature evolution is similar to the following heating processes.

Table 1. Test schemes

Case	Soil	Water content w(%)	Dry unit weight γ_d (kN/m^3)	Void ratio e	Degree of saturation S_r (%)	Primary temperature T_0 (°C)	Confining pressure σ'_3 (kPa)	Repeated number N	Temperature variation (°C)	Temperature variation of the second step(°C)
1	1, silty clay	25.1	15.5	0.70	96.9	25	50	6	25→50	
							100	6	25→50	
							150	6	25→50	
2	1, silty clay	22.1	16.5	0.61	97.8	25	50	6	25→75	
							100	6	25→75	
							150	6	25→75	
3	2, clay	29.7	15.1	0.85	95.1	20	50	3	20→50	50→80
							100	2	20→50	50→80
							150	2	20→50	50→80
4	3, red clay	47.0	11.9	1.25	99.2	20	50	1	20→40	
							50	1	20→50	
							50	1	20→60	
							50	1	20→80	
							50	1	20→90	

Pore pressure during two steps of undrained heating

The relationship of normalized pore pressure u/σ'_3 with the temperature of the clay (soil 2 in Table 1) for three confining pressures (σ'_3=50, 100, and 150 kPa) during two steps of undrained heating is also analyzed, and exhibits a pattern similar to that of the silty clay under repeated undrained heating (case 1 and case 2). In reality, the pore pressure induced by the second process of heating (50→80 ºC) still reaches a higher temperature (e.g., when σ'_3=50 kPa, u/σ'_3=0.84) although the specimens take on a slightly over-consolidated state due to having undergone a step of heating (20→50 ºC) and corresponding isothermal consolidation. The maximum pore pressure induced by the two steps of heating with isothermal consolidation between steps is lower than that induced by a single heating step (20→80 ºC) without the consolidation process.

Pore pressure of a red clay during undrained heating

For the red clay (soil 3 in Table 1), the pore pressure induced by heating also initially increases rapidly, subsequently reaching a higher value, and gradually assumes a steady state. Finally, the maximum normalized pore pressure reaches u/σ'_3=0.94 at a temperature of T=90 ºC, which means that the shear strength of the specimen nearly fails. It appears that the undrained thermal pressurization coefficient of the red clay (soil 3) is greater than that of the silty clay (soil 1) due to higher water content (w=47.0% and 22.1%, respectively, for soil 3 and soil 1). For example, when σ'_3=50 kPa and T=50 ºC, the normalized pore pressure of the red clay and the silty clay are u/σ'_3=0.65 and u/σ'_3=0.48, respectively.

Relationship between thermally induced pore pressures and temperature

The test results of the three soils show that the relationship between normalized pore pressure and temperature can be described by the following equation:

$$\frac{u}{\sigma'_3} = 1 - \frac{1}{1+\exp^{(T-\alpha)/\beta}} \qquad (1)$$

where T is the current temperature, and α and β are fitting parameters which determine the shape of the fitting curve.

The relationship given by Eq. (1) can be obtained using Matlabsoftware, a mathematical optimization analysis software package.

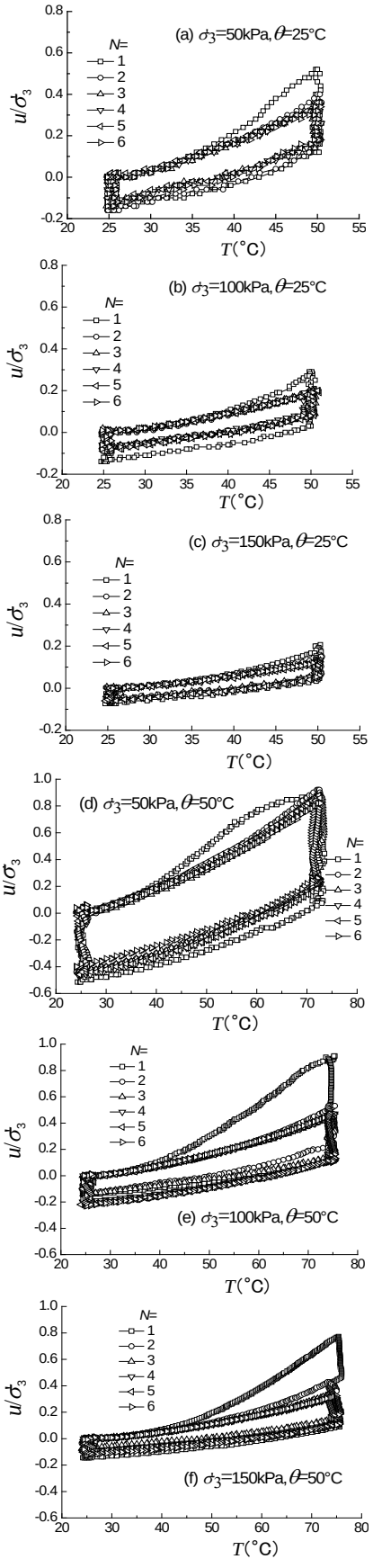

Fig. 1. Normalized pore pressure vs. temperature for various confining pressures and various temperature amplitudes.

Generally, optimization analysis is performed using the least squares method. Figure 2(a) illustrates the fitting relationship of the silty clay (soil 1) for case 2 when N=1, which shows that the evaluated results are in good agreement with the test data.

Here, when σ'_3=50, 100, and 150 kPa, then α=50.59, 58.15, and 64.39; β=8.20, 8.84, and 9.63; and the coefficient of determination is R^2=0.994, 0.997, and 0.999, respectively.

Parameters α and β are both linear with confining pressure, and can be written as

$$\alpha = a\sigma'_3 + b \quad (2)$$

$$\beta = c\sigma'_3 + d \quad (3)$$

where a, b, c and d are the parameters of soil properties.

Here, a=0.138, b=43.910, c=0.014 and d=7.461. The coefficients of determination are R^2= 0.997 and 0.996, respectively, for α and β.

Figure 2(b) illustrates the fitting curve for the red clay (soil 3), which also shows that the evaluated results agree with the test data. Here, α=44.59 and β=8.87, and the coefficient of determination R^2=0.982.

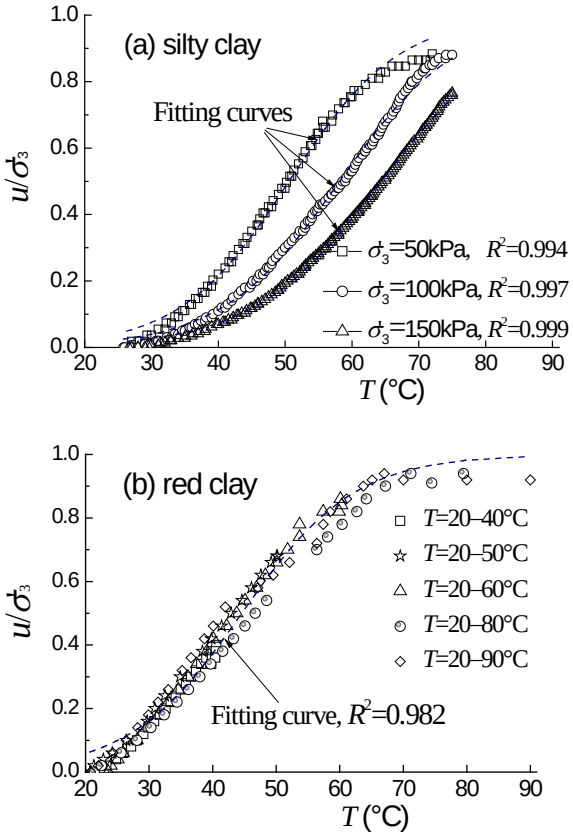

Fig. 2. Comparisons of evaluated pore pressure with measured values

Thermal consolidation volumetric strain

Figure 3 gives the fitting relationship between consolidation volumetric strain and thermally induced pore pressure for soils 1, 2 and 3 (see Table 1). Here, the consolidation volumetric strain is defined by $\varepsilon_v=\Delta V/V_0$, expressed as a percentage, with V_0 and ΔV being the specimen volume before consolidation and the amount of outflow pore water (both measured at primary temperature T_0), respectively.

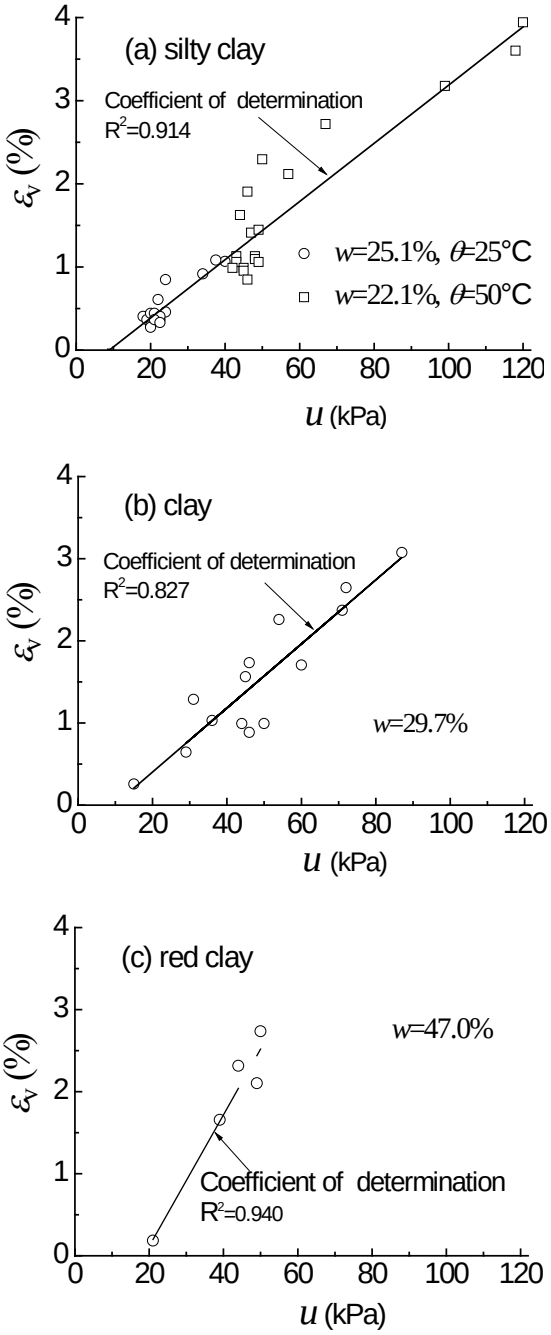

Fig. 3. Relationship between consolidation volumetric strains and pore pressure

Figure 3 shows that there are approximately linear relationships between volumetric strain and pore pressure, which is influenced by the specimens' water content, confining pressure, amplitude, and number of applied thermal loading cycles. The relationship is expressed as

$$\varepsilon_v = k(u - u_0) \quad (4)$$

where ε_v is the consolidation volumetric strain; u is the pore pressure induced by heating; and k and u_0 are fitting parameters.

For the silty clay, the obtained fitting parameters are k=0.035, u_0=8.91 and the coefficient of determination R^2=0.914 (Fig. 3(a)); for the clay, k=0.039, u_0=9.67 and R^2=0.827 (Fig. 3(b)); and for the red clay, k=0.080, u_0=18.51 and R^2=0.940 (Fig. 3(c)). In fact, the parameter k reflects the degree of variation in the amount of thermally induced volumetric strain. On the other hand, the parameter u_0 in Eq. (4) indicates an initial pore pressure. Figure 3 appears to show that the soils with a higher plasticity index or higher water content (for soil 3, I_p=32.6, w=47.0%) have greater thermal consolidation volumetric strain (i.e., a greater parameter k) than the soils with a lower plasticity index (e.g., for soil 1 and 2, I_p=13.8 and 19.1 , respectively; w=22.1–25.1% and w=29.7%).

CONCLUSION

(1) Generally, the normalized pore pressure increases as temperature increases, and decreases with the increase in confining pressure and repeated thermal loading cycles.

(2) Test results show that there are approximately linear relationships between consolidation volumetric strain and thermally induced pore pressure, which is influenced by the specimens' water content, confining pressure, amplitude and number of applied thermal loading cycles.

(3) An equation for describing the pore pressure induced by temperature and confining pressures is proposed. Additionally, the relationship between consolidation volumetric strain and thermally induced pore pressure is established

Acknowledgements: *This work is financially supported by the National Natural Science Foundation of China (51678043; 51478034), to which the authors are very grateful.*

REFERENCES

1. R.B. Hetnarski, J. Ignaczak, *Journal of Thermal Stresses*, **16**, 473 (1993).
2. H.R.Thomas, H.T. Yang, Y. He, P.J. Cleall, *International Journal for Numerical and Analytical Methods in Geomechanics*, **27**, 951 (2003).
3. H. Brandl, *Geotechnique*, **56**(2), **81,** 122 (2006).
4. A. Hüpers, A.J. Kopf, *Earth and Planetary Science Letters*, ***2*86**, 324 (2009).
5. M.V. Villar, R. Gomez-Espina, A. Lloret, *Journal of Rock Mechanics and Geotechnical Engineering*, **2**(1), 71 (2010).
6. B. Bai, X. Chen, *Journal of Geotechnical Engineering*, **33**(10), 1 (2011).
7. N. Khalili, A. Uchaipichat, A.A. Javadi, *Mechanics of Materials*, **42**, 593 (2010).
8. S. Ghabezloo, J. Sulem, *Italian Geotechnical Journal*, **1**, 29 (2010).
9. M. Monfared, P. Delage, J. Sulem, M. Mohajerani, A.M. Tang, E. De Laure, *International Journal of Rock Mechanics and Mining Sciences*, **48**, 637 (2011).
10. G. Yilmaz, *Scientific Research and Essays*, **6**(9): 1928 (2011).
11. H.M. Abuel-Naga, D.T. Bergado, A. Bouazza, *International Journal of Geomechanics*, **8**(2), 114 (2008).
12. L. Laloui, C. Cekerevac, *Computers and Geotechnics* **30**, 649 (2003).
13. V.R. Ouhadi, R.N. Yong, A.R. Goodarzi, M. Safari-Zanjani, *Applied Clay Science* , **47**, 2 (2010).
14. R.G. Campanella, J.K. Mitchell, *Journal of Soil Mechanics and Foundation Engineering Division*, **94**(3), 709 (1968).
15. V.V. Palciauskas, P.A. Domenico, *Water Resources Research*, **18**(2), 281 (1982).